Materials Horizons

ROYAL SOCIETY OF CHEMISTRY

COMMUNICATION

View Article Online
View Journal | View Issue

Cite this: *Mater. Horiz.*, 2022, 9, 3039

Received 19th July 2022,
Accepted 21st September 2022

DOI: 10.1039/d2mh00907b

rsc.li/materials-horizons

A salt-triggered multifunctional smart window derived from a dynamic polyampholyte hydrogel†

Jing Guo,‡ Shanshan Wu,‡ Yilei Wang, Jinhui Huang, Hui Xie * and Shaobing Zhou *

Hydrogel smart windows are promising candidates for the automatic modulation of light transmittance through thermo-, humidity-, and electrochromic mechanisms. However, thermo- and humidity-triggered hydrogel smart windows are usually passively controlled and are not convenient for achieving active actuation; electrochromic windows require complex assembly and energy input. In addition, existing hydrogel smart windows are susceptible to physical damage, which may significantly shorten their working life. Herein, a salt-triggered polyampholyte hydrogel (PAH) is developed as a novel smart window with active and facile actuation as well as self-healing ability. The dynamic ionic bonds in PAH can reversibly disassociate and reform in alternate aqueous sodium chloride solution (NaCl(aq.)) and H_2O, accounting for the reversible transparency-shifting and efficient modulation of light transmittance. PAH also enables patterning through precisely localized treatment with NaCl(aq.), which is useful for one-time information input/storage. Information encryption can be further realized by embedding PAH into an inherently transparent hydrogel or pasting it on an information carrier; the visibility of information is in line with the transparency-shifting of PAH. Moreover, the dynamic ionic bonds can endow the PAH-derived hydrogel smart window with self-healing and automatic damage-repairing abilities without sacrificing light modulation. Thus, salt-triggered PAH provides a new idea for designing actively actuating hydrogel smart windows with multifunctionality.

New concepts

This study provides a new concept to design multifunctional smart windows by salt-triggered dynamic chemistry using a polyampholyte hydrogel (PAH). Hydrogel smart windows are promising candidates for automatically modulating light transmittance through thermo-, humidity- and electrochromic mechanisms that are either passively controlled or require an extra energy input; in addition, hydrogels can be susceptible to physical damage, which may significantly shorten their working life. Herein, this work proposes PAH as an emerging material platform to develop hydrogel smart windows with active and facile light modulation and self-healing capacity. The transparency-shifting behavior of PAH coincides with the dynamic nature of ionic bonds that is regulated by alternate H_2O and aqueous sodium chloride solution (NaCl(aq.)), and this is imporatant for light modulation; besides, this work demonstrates the feasibility of endowing the derived smart window with the extra advancement of on-demand information-provision management by either precisely localized patterning of PAH, embedding PAH into a transparent hydrogel, or pasting PAH on information carriers. Furthermore, the dynamic ionic bonds enable the automatic healing of damage without any sacrifice in light modulation. Given the wide availability of dynamic chemistries, this work will inspire the design of actively actuating hydrogel smart windows with multifunctionality.

Introduction

Smart windows are emerging materials that can dynamically regulate light transmittance in response to external stimuli, such as temperature, electricity, and humidity,[1] and through this light modulation process, they can achieve the goals of energy-efficient and sustainable development in modern buildings.[2,3] Among the materials used for smart windows, hydrogels have garnered increasing attention in recent years. Hydrogels are a type of highly hydrated and flexible three-dimensional polymer network containing abundant water; owing to the characteristics of solid and liquid, hydrogels are suitable candidates for soft smart windows. For smart windows, hydrogels enable different mechanisms for achieving high contrast in transparency/opacity, and they can naturally match the goal of light transmittance modulation. In addition, hydrogels have the advantages of facile design, fabrication, and operation.[4] Numerous studies have been conducted on hydrogel-derived smart windows, and three working mechanisms have been developed: thermo-,[5,6] humidity-,[7] and electrochromic mechanisms.[8,9] Thermo- and humidity-chromic

Key Laboratory of Advanced Technologies of Materials, Ministry of Education of China, School of Materials Science and Engineering, Southwest Jiaotong University, Chengdu 610031, China. E-mail: huixie@swjtu.edu.cn, shaobingzhou@swjtu.edu.cn

† Electronic supplementary information (ESI) available. See DOI: https://doi.org/10.1039/d2mh00907b

‡ These authors contributed equally to this work.

hydrogel smart windows are activated by the surrounding environmental conditions in a passive manner, and achieving active modulation is challenging. Electrochromic hydrogel smart windows can be actively controlled by manually applying voltage; however, they require additional energy input and complex assembly of equipment. Therefore, hydrogel smart windows that can be actively and easily actuated are highly desirable.

Among hydrogel smart windows, thermochromic windows are the most popular.[10] They exhibit transparency changes in response to changes in the surrounding temperature. Hydrogels with a lower critical solution temperature (LCST) are often used to design thermochromic hydrogel smart windows, such as hydroxypropyl cellulose,[11] poly(*N*-vinylcaprolactam)[12] and poly(*N*-isopropylacrylamide) (PNIPAm).[13–18] The modulation of light transmittance relies significantly on the changes in the surrounding temperature. When the external temperature is higher than the LCST, the polymer chains in the hydrogel aggregate and block the incident light, resulting in low transmittance; when the temperature decreases to less than the LCST, the aggregation is weakened, resulting in high transmittance. Recently, Long *et al.*[14] developed a PNIPAm (LCST = 32.5 °C)-based hydrogel smart window, which exhibited 90% luminous transmittance and 68.1% solar modulation; an additional function of heat storage was also realized, which can further decrease energy consumption. Humidity in the external environment can also be used as an external stimulus to realize light modulation. As both thermo- and humidity-chromic mechanisms can be designed to respond to stimuli from the surroundings, the modulation of light transmittance should be regarded as passive actuation; this makes it challenging to meet personalized needs for manually adjusting incident light, that is, active actuation.

To achieve active modulation of light transmittance, electrochromic hydrogel smart windows have been proposed.[19–22] In an indirectly electrochromic hydrogel smart window, incorporating a conductive electrode capable of electro-thermal conversion into a thermochromic hydrogel is a feasible strategy. Long *et al.*[19] assembled a transparent conductive electrode in a grid or honeycomb structure along with a thermochromic PNIPAm hydrogel into an electrochromic device; they achieved an optimal transparent/opaque contrast of 70% by manually applying voltage. Alternatively, a direct electrochromic effect can be achieved by using an inherent electrochromic component. Wang *et al.*[20] reported a three-layered device comprising a lithium chloride-containing polyacrylamide hydrogel (PAAm-LiCl), F-doped SnO_2 (FTO) and tungsten oxides (WO_{3-x}); PAAm-LiCl-based hydrogel smart windows exhibited a significant colour change with a large modulation of light transmittance ($\leq$70%). Electrochromic hydrogel smart windows can be actively controlled; however, they require device assembly and auxiliary equipment for additional energy input, which makes the process complex and is not beneficial for energy-saving actuation.

In this study, we propose a salt-triggered polyampholyte hydrogel (PAH)-derived hydrogel smart window. The ionic bonds in PAH were salt-triggered, and this process was synergistically involved in transparency-shifting, which was unlike the widely reported thermochromic feature of PAH.[23] Therefore, PAH can enable the design of a new hydrogel smart window with active actuation and facile operation for modulating light transmittance. Furthermore, PAH can be patterned by precisely localized treatment of the aqueous sodium chloride solution (NaCl(aq.)). This was demonstrated to be useful for one-time information input/storage, and information encryption could be further realized by embedding PAH into a conventional transparent hydrogel, paving the way for developing information-providing hydrogel smart windows. Additionally, PAH exhibited self-healing, which provided the functions of automatically repairing damage without any sacrifice in light modulation. Therefore, PAH endowed the derived hydrogel smart window with multifunctionality.

Results and discussion

Preparation and characterization of PAH

PAH was prepared from a cationic monomer (methyl chloride quaternized *N,N*-(dimethylamino)ethylacrylate, DMAEA-Q), an anionic monomer (sodium *p*-styrenesulfonate, NaSS) and a physical cross-linker (2-ureidoethyl methacrylate, UM), as shown in Fig. 1a. The oppositely charged ionic monomers formed ionic bonds, and the UM units donated hydrogen bonds; consequently, the fabricated PAH should be a physical hydrogel. The chemical structure of PAH was characterized by Fourier transform infrared spectroscopy (FT-IR), and the peaks at approximately 1571 cm^{-1} (N–H), 1488 cm^{-1} (C–N^+), and 1124 cm^{-1}, 1035 cm^{-1} and 1008 cm^{-1} (C–SO_3^-) were derived from the initial monomers UM, DMAEA-Q and NaSS, respectively (Fig. S1 and S2, ESI†).

Swelling tests were then performed to examine the formation of physical networks. Fig. S3 (ESI†) shows that the swelling ratio (S (%)) of PAH in NaCl(aq.) was much higher than that in pure water (H_2O). Generally, a polymer network with a higher cross-linking density possesses a lower swelling ratio in a suitable solvent and *vice versa*; therefore, the dramatic increase in S (%) strongly reflects the dissociation of gel networks in PAH in NaCl(aq.). In addition, PAH did not dissolve in NaCl(aq.), confirming that the hydrogen bonds could serve as permanent netpoints for PAH during NaCl(aq.) treatment to maintain the gel network and prevent collapse. Given the importance of the dynamic nature of ionic bonds in the current study, additional swelling tests were performed by immersing PAH in NaCl(aq.) and H_2O alternately (Fig. S4, ESI†). Here, the equilibrium weight of PAH in H_2O, instead of the dried PAH, was defined as the base weight to calculate S (%) of the gel in NaCl(aq.) and H_2O alternately. Fig. S4 (ESI†) clearly shows that S (%) in NaCl(aq.) was higher than that in H_2O in every cycle, which also proves the breakage of the ionic bonds of PAH in NaCl(aq.).

Another piece of evidence for the change in the network density of PAH was the difference in pore sizes between

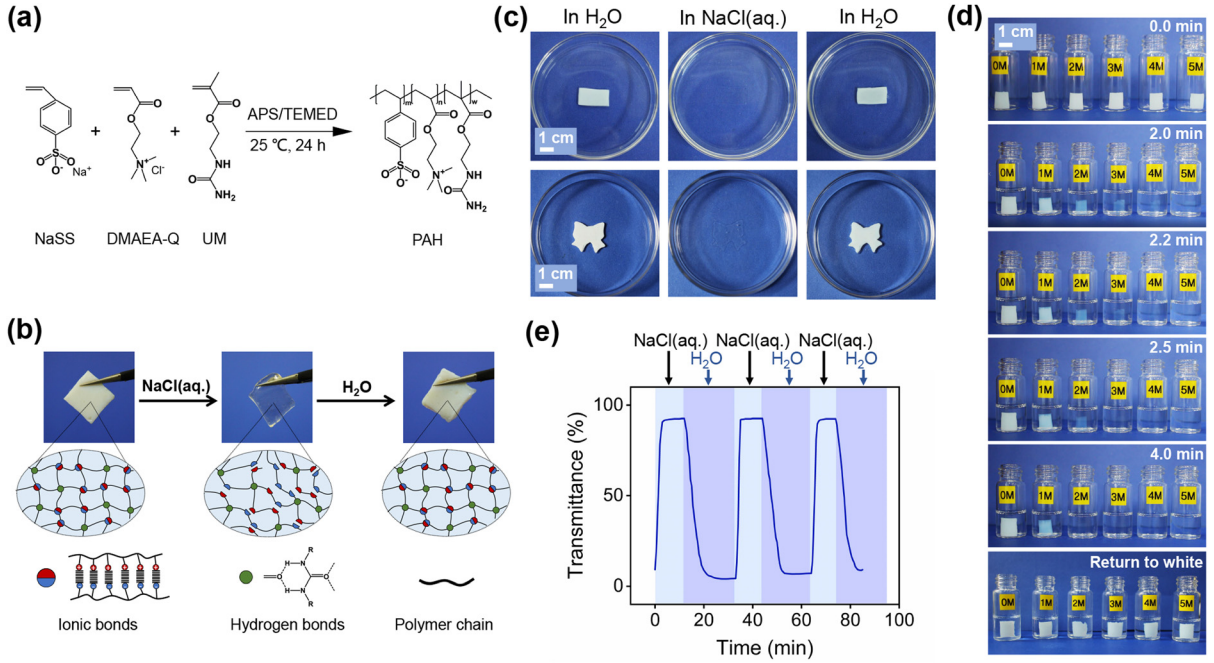

Fig. 1 (a) Copolymerization of the cationic and anionic monomers (NaSS and DMAEA-Q) and the cross-linker (UM) for the preparation of PAH. (b) Pictures showing PAH in white (opaque) and transparent states when immersing in H_2O and NaCl(aq.), respectively, and the proposed dynamic nature of ionic bonds. (c) Optical images of the hydrogel from white to transparent and return to white in H_2O and NaCl(aq.), the scale bar is 1 cm. (d) Comparison of the transparency-shifting process of PAH in 0, 1, 2, 3, 4, and 5 M NaCl(aq.). The size of the PAH specimen was 10 mm × 10 mm × 0.5 mm, and the scale bar is 1 cm. (e) Change in transmittance (at 550 nm) of PAH during H_2O/NaCl(aq.) treatments recorded by UV-vis. The size of the PAH specimen was 40 mm × 10 mm × 2 mm.

specimens in H_2O and NaCl(aq.). The scanning electron microscopy (SEM) images indicated that the specimen treated with NaCl(aq.) possessed larger pores after freeze-drying (Fig. S5, ESI†). Generally, hydrogels with higher densities result in smaller pores after freeze-drying and *vice versa*; therefore, the results of SEM undoubtedly confirmed the dissociation of gel networks of PAH. As hydrogen bonds are not sensitive to NaCl(aq.), the dissociation of gel networks can only be ascribed to the dissociation of ionic bonds in PAH. Notably, the as-prepared white PAH soaked in deionized water turned transparent after being transferred to NaCl(aq.), which laid the foundation for engineering salt-triggered PAH as a new type of hydrogel-derived smart window. The transparency-shifting of PAH is systematically investigated in the following sections.

Transparency-shifting of PAH

As shown in Fig. 1b and c, the prepared PAH was white after soaking in deionized water and after being treated with NaCl(aq.), it quickly changed from opaque to transparent. The transparency-shifting was synergistic with the varying light transmittance, which is the core of a smart window. This phenomenon inspired us to design a hydrogel smart window using salt-triggered modulation. First, we investigated whether the concentrations of NaCl(aq.) could affect the transparency-shifting of PAH. A series of NaCl(aq.) solutions with different concentrations (0–5 M) were set to study the difference in transparency-shifting; both the size of the PAH specimen and the volume of the solution were unchanged for the parallel study. Notably, the concentration of saturated NaCl(aq.) at 25 °C is approximately 5.43 M; thus, the maximum concentration in our experiments was set as 5 M. The time required for transparency-shifting was found to be highly dependent on the NaCl(aq.) concentration; the higher the salt concentration, the shorter the transition time. For instance, PAH required 4 min to become transparent when soaked in 2 M NaCl(aq.), whereas, for 5 M NaCl(aq.), this process was completed within 2 min. For a certain immersion time (4 min), the specimen immersed in NaCl(aq.) ($\geq$2 M) was transparent, whereas the others were not, even though all of them could return to white after being transferred to H_2O (Fig. 1d and Movie S1, ESI†). As stated previously, the transparency-shifting of PAH is dominated by ionic bonds. Even though the ionic bonds could easily dissociate and weaken the gel networks of PAH, the hydrogen bonds inside would be sufficiently stable to maintain the macroscopic morphology during salt stress. Considering the time and efficiency of the transparency-shifting process, 3 M NaCl(aq.) was selected for the investigations described in the following sections.

Subsequently, we conducted a quantitative study of circular transparency-shifting, which could reflect the reversibility of hydrogel smart windows in light transmittance modulation. The transmittance of PAH during alternate H_2O/NaCl(aq.) treatment was measured by ultraviolet-visible (UV-vis) analysis, and the transmittance at a certain wavelength in the visible light range (550 nm) along with the time increment is shown in Fig. 1e. Generally, 100% and 0% transmittances are fully

transparent and opaque, respectively, and the change in transmittance reflects the transparency-shifting trend. After fully soaking in H_2O, PAH was white with a 4% transmittance and then exhibited a gradual increase in transmittance to 92% until reaching equilibrium in NaCl(aq.) (3 M), indicating an efficient opaque-to-transparent transition, which took approximately 10 min. When PAH was transferred from NaCl(aq.) to H_2O, the transmittance dramatically decreased to the initial level ($\sim$4%) within 20 min, indicating a light transmittance modulation efficiency of 88% owing to the transparent-to-opaque shift of PAH. The light modulation efficiency can be regarded as excellent compared to most of the reported literature, as summarized in Table S1 (ESI†). The transparent-to-opaque transition should be activated by the reassembly of ionic bonds and *vice versa*. As reported in Gong's previous work,[24–26] the ionic bonds of the gel were destroyed by the invasion of abundant Na^+ and Cl^- in NaCl(aq.), whereas the small co-ions and counterions in PAH diffuse into the water during soaking. The aforementioned two processes can be attributed to the difference in the concentration and solution environment of the gel. Therefore, the opaque-to-transparent time was shorter than that for the reverse process, which could be attributed to the infiltration velocity of Na^+ and Cl^-. The differential concentrations of PAH and NaCl(aq.) should be greater than that between the transparent PAH and H_2O. The excellent reversibility of the transparency-shifting in successive H_2O/NaCl(aq.) treatment cycles was confirmed by the reversible change of transmittance in the same range, and surprisingly, the time for each state of circular transparency-shifting was almost constant, further demonstrating excellent reversibility.

The underlying mechanism of salt-triggered transparency-shifting can be explained by the change in the aggregation state of the polymer chains. PAH in its initial state is supposed to be physically cross-linked by both ionic and hydrogen bonds; the gel networks are in high density, and the polymer chains are also densely entangled, making it difficult for natural light permeation and finally resulting in an optically opaque state. When immersed in NaCl(aq.), the dissociation of ionic bonds in PAH leads to partial rupture of the gel networks and loss of polymer chain entanglement, which can permeate easily and eventually generate an optically transparent phenomenon. In brief, the reversible transparency-shifting of PAH could enable the design of a new type of hydrogel smart window with an active salt-triggered mechanism.

PAH-derived salt-triggered smart windows

The salt-triggered transparency-shifting of PAH has been demonstrated in previous sections, which inspired us to engineer it as a new prototype of hydrogel smart windows. First, the effect of PAH on the transmittance of a real landscape was investigated. A piece of PAH was placed in a cuvette, and the transparency-shifting of PAH during H_2O/NaCl(aq.) treatment enabled the control of an individual's spotting of objects (Fig. 2a). Then, our main objective was to establish a prototype of a PAH-derived smart window based on the aforementioned achievements, and an illustration of the prototype is presented in Fig. 2b. Briefly, a piece of square PAH (thickness: 1.0 mm) was assembled between two glass plates as the light modulation layer, and a tailored silicone gasket (thickness: 2.0 mm) was placed between the glass plates as the interlayer to provide a gap for adding and removing liquid (H_2O or NaCl(aq.)) according to the requirements for transmittance modulation. The function of the PAH-derived smart window is to control the visibility of an object *via* the salt-triggered transparency-shifting of PAH by alternately applying H_2O/NaCl(aq.). Using sunflower as a model, the working module of the proposed hydrogel smart window is shown in Fig. 2c. The assembled window was initially white (optically opaque) and the sunflower behind the window was invisible; thus, for an individual, it could be difficult to get a distinct picture. When injecting NaCl(aq.) into the window, PAH became transparent, a shielded sunflower appeared, and an individual could readily capture the picture. Upon replacing the NaCl(aq.) with H_2O, the window became opaque and the sunflower became invisible again (Movie S2, ESI†). These processes can be performed repeatedly, and the modulation of light transmittance is controlled manually and should be regarded as actively actuating.

In comparison with conventional hydrogel smart windows based on thermo-, humidity-, and electrochromic mechanisms, the proposed salt-triggered PAH-derived smart window could enable the active starting of the transparency-shifting process by easily adjusting the immersing solvents, H_2O and NaCl(aq.). Meanwhile, the entire process may only involve a simple device, for example, some sort of flushing system. Therefore, the PAH smart window proposed in this study possesses distinct advantages, including on-demand control and facile operation, which will be beneficial for a sustainable future.

Patterning and embedding of PAH for information-providing smart windows

In previous sections, PAH has been demonstrated to work as a new type of hydrogel smart window that could be actively modulated by salt, and its transparency-shifting endowed the on-demand control of the visibility of objects. Here, we investigated whether we could achieve more joint add-values on a PAH-derived smart window platform beyond basic transparency-shifting. Recently, smart windows have been proposed to be used as information carriers,[27] for instance, in information storage and encryption. First, we assumed that the dynamic ionic bonds of PAH could be selectively ruptured once the localized NaCl(aq.) treatment could be realized, and consequently, patterns representing certain information would be created as a result of distinct boundaries of opaque and transparent areas. Following this idea, a series of experiments were conducted. As shown in Fig. 3a, a silicone gasket with a tailored hollow structure was tightly covered on the surface of PAH (thickness: 0.5 mm). Then, NaCl(aq.) was slowly poured into the hollow area. The NaCl(aq.) penetrated the inside of PAH in a vertical direction, instead of horizontally diffusing to the shielding area. After removing the mask, the corresponding patterns observed in the area treated with NaCl(aq.) became transparent, whereas the shielding area remained white, as shown in Fig. 3b.

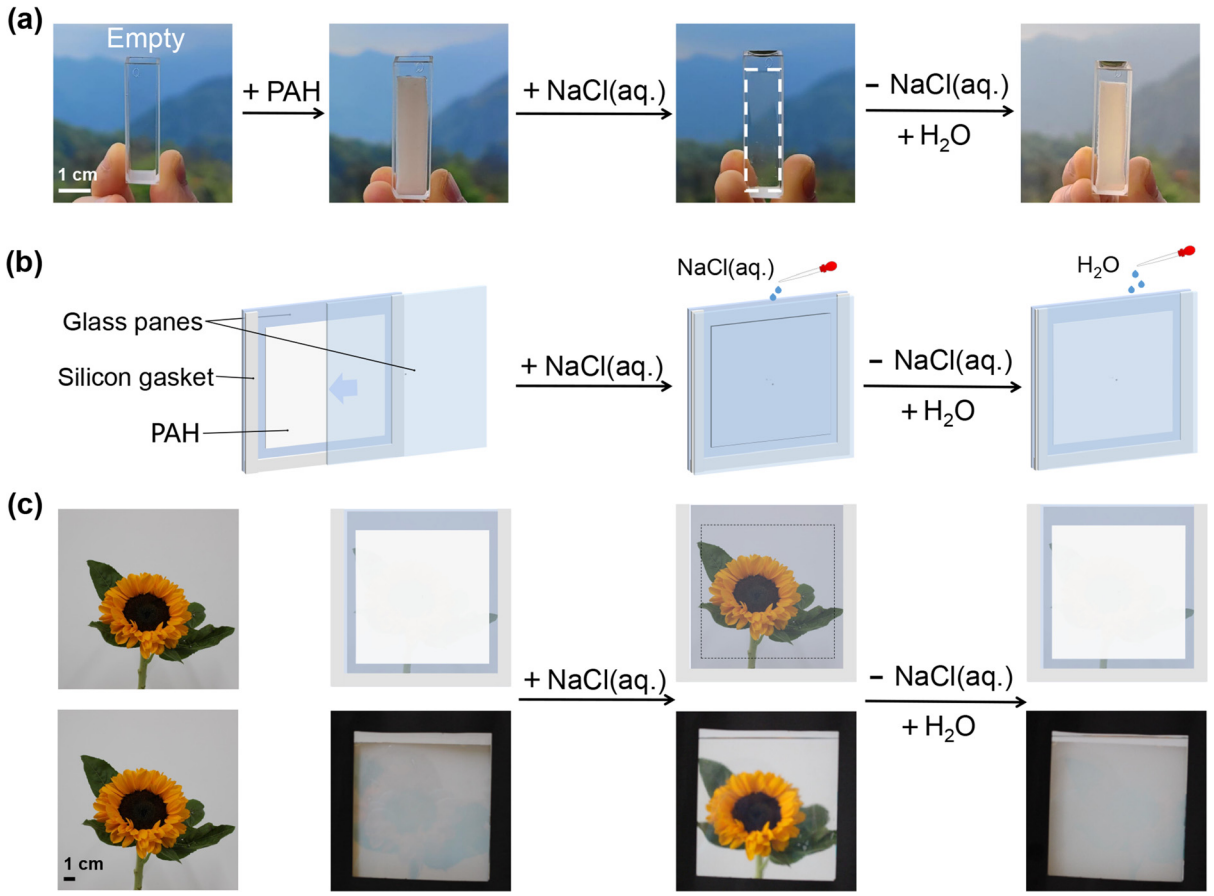

Fig. 2 (a) Transmittance of the landscape through PAH (in cuvette), the scale bar is 1 cm. (b) Graphic illustration of the prototype of a PAH-derived smart window. The thicknesses of the PAH film and the silicone gasket were 1.0 and 2.0 mm, respectively. (c) Proof-of-concept of the proposed hydrogel smart window in modulating natural light transmittance. The model presented in the picture is fresh sunflower, the scale bar is 1 cm.

Notably, the time for patterning was only 2 min; therefore, this process should be regarded as facile and time-saving.

The described process refers to the information input/storage of the hydrogel smart window. However, it was still difficult to achieve encryption during reversible transparency-shifting as either NaCl(aq.) or H_2O led to the disappearance of the boundaries between opaque and transparent areas (Fig. 3b). Briefly, the patterned PAH was opaque (in H_2O) or transparent (in NaCl(aq.)), and the created pattern disappeared. In other words, PAH became homogeneous, enabling repeated patterning and information input/storage. Nevertheless, this simple patterning could be regarded as a strategy to realize one-time information provision in PAH-derived smart windows.

As a proof-of-concept for an information-encrypting hydrogel smart window, PAH was employed as an embedding component in a conventional polyethylene glycol (PEG) hydrogel, which is inherently transparent. It was expected that the PAH component would be assembled into certain patterns representing specific information and that the transparency-shifting of PAH regulated by H_2O/NaCl(aq.) would lead to visibility control of the pattern (information), while the insensitive PEG component would maintain the macroscopic morphology of the window. As shown in Fig. 4a, PAH (either one piece or more) (thickness: 0.5 mm) was assembled into different patterns (shapes or letters), such as maple leaf and SWJTU1896, followed by the addition of poly(ethylene glycol)diacrylate aqueous solution (PEGDA(aq.)); eventually, an encapsulated hydrogel smart window could be obtained after cross-linking at room temperature and fully soaking in H_2O. The fabrication process should be regarded as information input and storage, and the information encryption feature can be reflected by the reversible opaque–transparent transformation. The samples and their encryption processes are shown in Fig. 4b and Movie S3, ESI.† The information (maple leaf or SWJTU1896) was visible (unencrypted) when immersed in H_2O as PAH was white. After being transferred to the NaCl(aq.) medium, the information became invisible (encrypted) as PAH became transparent, and when immersed in H_2O, the information appeared again (decrypted) as PAH returned to its opaque state. The entire information unencrypted–encrypted–decrypted process was in tune with the transparency-shifting of the PAH component, which is supposed to be repeatable for many cycles.

In brief, simple patterning of PAH using localized NaCl(aq.) treatment could ensure one-time information input/storage for the derived hydrogel smart window. Information encryption could be further realized by embedding PAH into an inherently

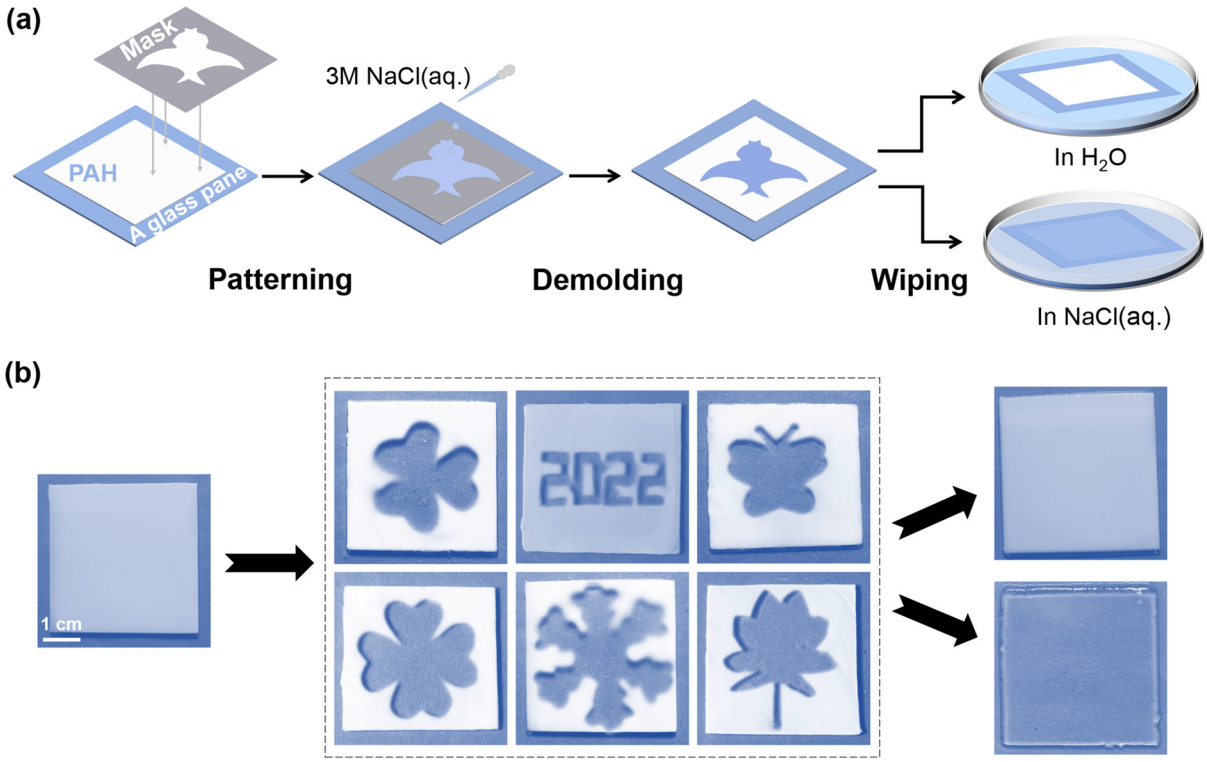

Fig. 3 (a) Schematic demonstration of patterning on the gel through NaCl(aq.) painting. (b) Images of different painted patterns on PAH, the scale bar is 1 cm.

transparent PEG hydrogel, and the visibility of information (PAH component) was in line with reversible transparency-shifting regulated by H_2O and NaCl(aq.).

PAH as an adhesive and self-healing smart window

The great potential of salt-triggered PAH for emerging smart windows was proved by the discussed results. In this study, we focused on the additional functions of PAH for multifunctional hydrogel-derived smart windows. Supramolecular polymeric hydrogels have been widely studied as smart adhesives,[28–31] and this inspired us to examine the adhesion property of the proposed PAH, which is intrinsically a supramolecular hydrogel. We assumed that an adhesive hydrogel smart window would enable the modulation of see-through information on a large number of substrates. First, the adhesion ability of PAH was demonstrated by a series of experiments involving different kinds of substrates, plastics (goggles), glass (bottle) and metal (pen) (Fig. 5a), and Fig. 5b presents the adhesive strength of PAH treated with H_2O/NaCl(aq.) on plastic, glass and metal substrates measured using the lap shear test.[31] The qualitative and quantitative measurements of the adhesion properties demonstrated that PAH could adhere tightly to these substrates in both H_2O and NaCl(aq.), which indicated the stable long-term adhesion of PAH during cyclic H_2O/NaCl(aq.) treatment.

Then, our attention was paid to the control of the visibility of the information on the substrates. The pen with our university name in Chinese, ''Southwest Jiaotong University,'' was carefully covered by PAH, and the printed Chinese characters were invisible after soaking in H_2O; the hydrogel became transparent after immersing in NaCl(aq.), and the characters could be captured by an individual (at the bottom of Fig. 5a). This process could be regarded as the modulation of a see-through information display in which the salt-triggered transparency-shifting of PAH played a dominant role. The adhesive feature of PAH would make the derived smart window applicable to various substrates for on-demand light management, leading to a versatile hydrogel smart window.

As the core of the proposed PAH-derived hydrogel smart window, transparency-shifting has been assigned to the dynamic nature of ionic bonds, and our main interest was then focused on the possibility of making the proposed hydrogel smart window more sustainable using the inherently dynamic feature of PAH. Generally, hydrogels are susceptible to external forces, particularly sharp subjects, which can weaken the properties of hydrogels and thus reduce their working span. This situation is also applicable to hydrogel smart windows. Herein, the self-healing concept[32] was proposed to achieve this goal using the salt-triggered dynamic ionic bonds in PAH. In agreement with the function of the smart window, the self-healing of PAH in its optically transparent state was examined. As shown in Fig. 5c, the salt-soaked PAH (size: 40 mm × 20 mm × 2 mm) was in a transparent state and then cut into two parts, which could be healed after contact with each other at room temperature for a short time (within 5 min). The healed PAH was stretchable and the crack did not propagate, indicating a high healing efficiency. Besides, we examined Young's modulus of the original and healed PAH samples. Fig. 5d shows that the

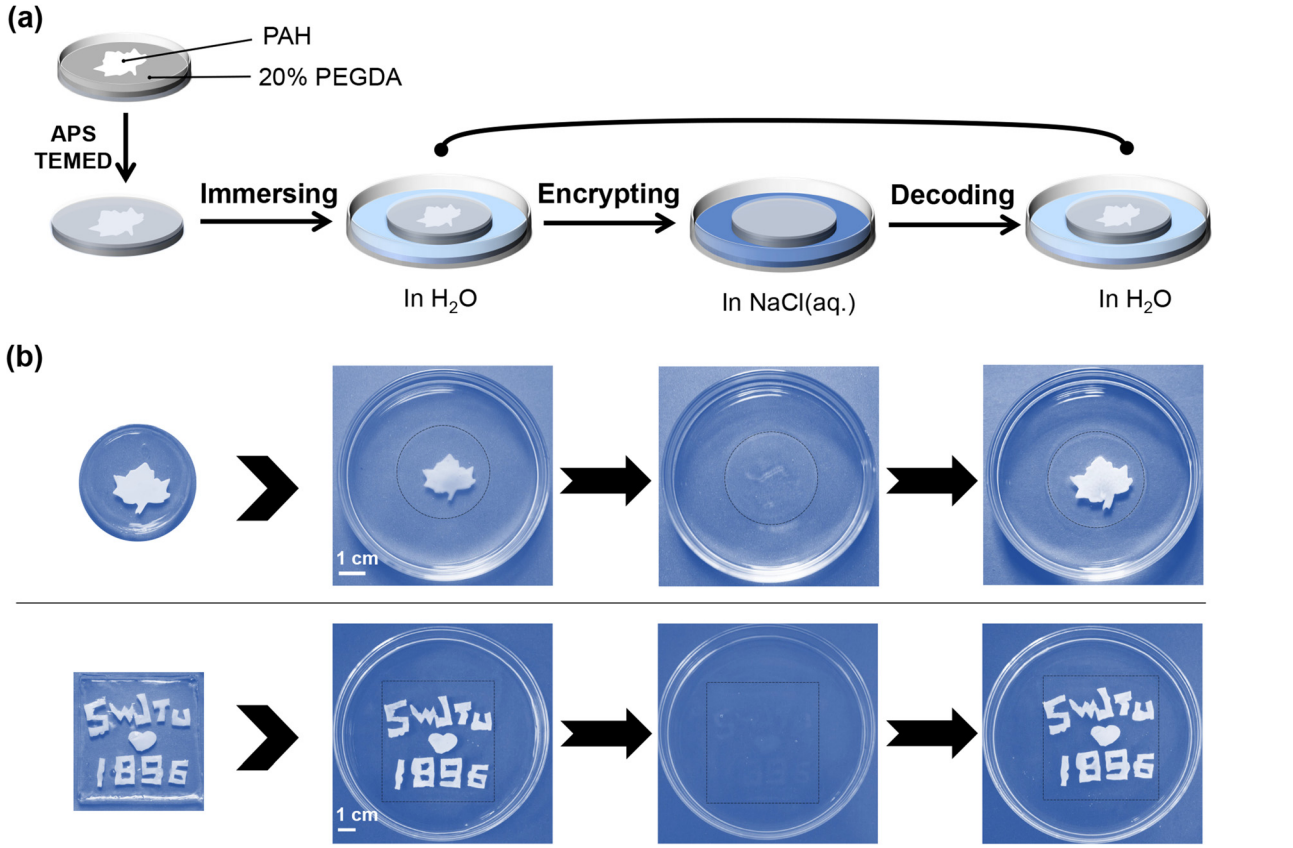

Fig. 4 (a) Schematic of fabrication of an encapsulated hydrogel. PAH was used as an information carrier and embedded into the transparent PEG hydrogel. (b) Optical images showing information encryption for the encapsulated hydrogel, the scale bar is 1 cm.

modulus before self-healing and the modulus after self-healing were almost the same. Furthermore, the cross-sectional morphology observed by SEM indicated the excellent healing of fractures without obvious cracks at the interfaces (Fig. S6, ESI†). In addition, the self-healing process does not affect the transparency-shifting of PAH in H_2O and NaCl(aq.), that is, the core function of a smart window. Overall, the self-healing ability of PAH not only makes it possible for the derived smart window to automatically repair damage and lengthen its working life but also lays the foundation for designing smarter and multifunctional hydrogel windows.

Conclusion

In conclusion, a novel salt-triggered multifunctional hydrogel smart window derived from PAH was developed. The transparency-shifting of PAH coincided with the dynamic feature of ionic bonds that could be regulated by treatment with H_2O and NaCl(aq.); this process can be regarded as actively and facilely modulating light transmittance. The PAH-derived hydrogel smart window exhibited a high light transmittance modulation efficiency of 88%, which was excellent compared to those of most of the hydrogel smart windows reported in the literature. Moreover, the dynamic ionic bonds in PAH endowed the derived smart window with multifunctionality. By precisely implementing the NaCl(aq.) treatment through certain masks, PAH was patternable, leading to a one-time information input/storage ability, as the information could be wiped by immersing either in NaCl(aq.) or H_2O. Information encryption was further realized by embedding PAH into an inherently transparent PEG hydrogel, and the visibility of embedded information was still in line with the transparency-shifting of PAH, facilitating the encoding and decoding of information on demand. In addition, PAH could adhere to various substrates, enabling the management of information provision beyond light modulation. Besides, dynamic ionic bonds in PAH provided a smart window with self-healing capacity without sacrificing light modulation. The salt-triggered multifunctional hydrogel smart window derived from PAH can inspire the design of smarter smart windows for a sustainable future.

Experimental section

Materials

Methyl chloride quaternized *N,N*-(dimethylamino)ethylacrylate (DMAEA-Q, 80 wt% in water, Best-Reagent), sodium *p*-styrenesulfonate (NaSS, 90%, Aladdin), 2-isocyanatoethyl methacrylate (98%, Aladdin), ammonium hydroxide (18%, Kelong), ammonium persulfate (APS, Aladdin), *N,N,N′,N′*-tetramethylethylenediamine (TEMED, Adamas), and sodium chloride (NaCl, General-reagent) were used as received. 2-Ureidoethyl

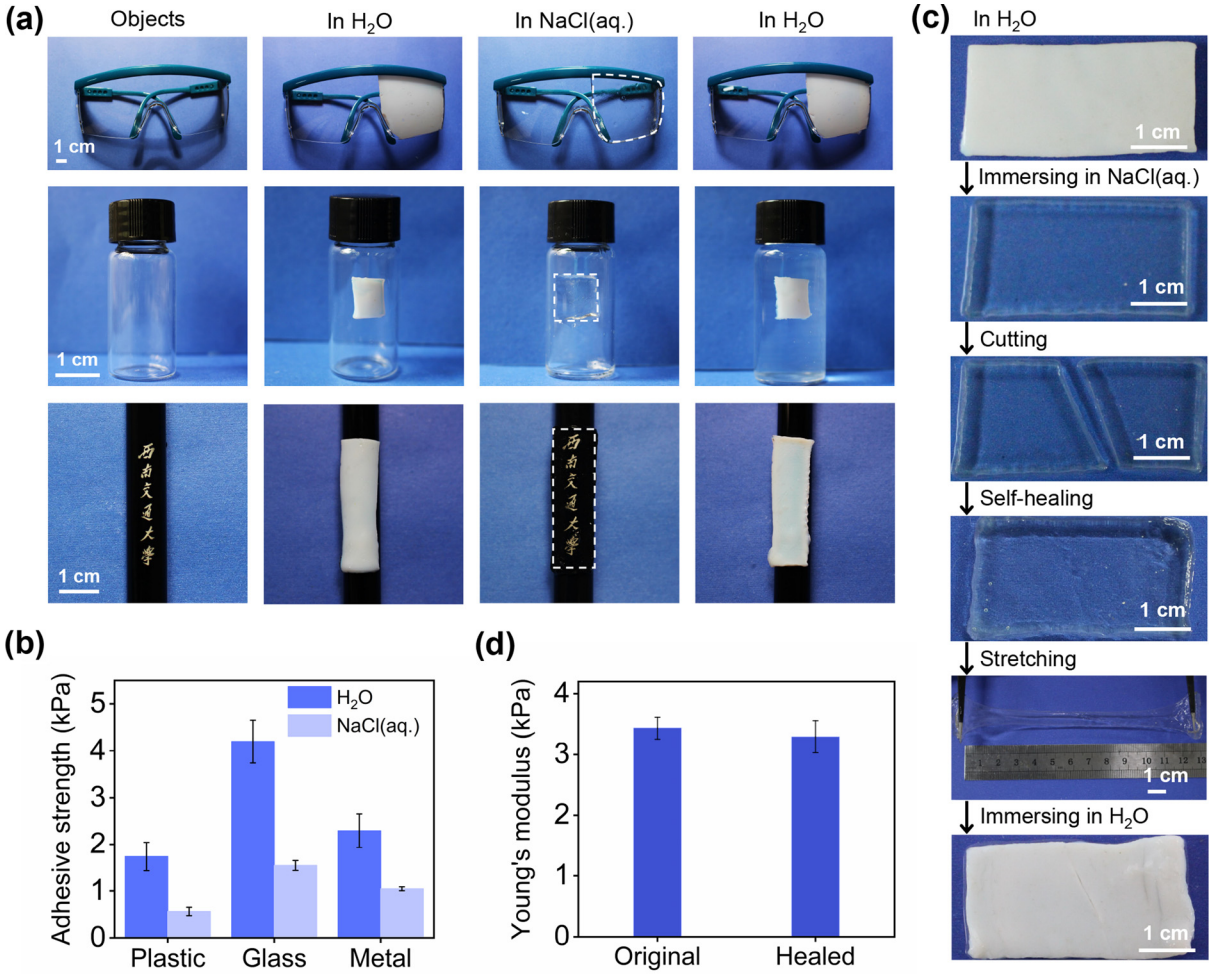

Fig. 5 (a) Pictures showing PAH adhering to different substrates, plastics, glass, and metal. The objects were goggles, a bottle and a pen, the scale bar is 1 cm. (b) The adhesive strength of PAH treated with H_2O and NaCl(aq.) on plastic, glass and metal substrates. (c) The self-healing ability of PAH, the scale bar is 1 cm. (d) Young's modulus of the original and healed PAH samples.

methacrylate (UM) was synthesized using the method reported in the previous research.[33] Pure water (H_2O) was prepared in the laboratory.

Synthesis of PAH

PAH was prepared through a modified process according to a previously described method.[26] First, the cation monomer DMAEA-Q (0.96 M), anionic monomer NaSS (1.04 M) and the physical cross-linker UM (1 mol% relative to the total monomer concentration) were fully dissolved in 0.5 M NaCl(aq.) as the precursor solution. Then, APS (1 mol% relative to the total monomer concentration) and TEMED were added to the homogeneous precursor solution. Next, nitrogen was aerated into the precursor solution to replace the dissolved oxygen, which was beneficial for radical polymerization. Finally, the aqueous solution was injected into a customized mold composed of two transparent glass panes (80 mm × 80 mm × 3 mm) and a silicon spacer with different thicknesses (0.5, 1.0, and 2.0 mm), and the reaction was maintained at room temperature for 24 h. After radical polymerization was completed, the as-prepared hydrogels were dialyzed in pure water for at least one week.

Fourier transform infrared spectroscopy (FT-IR)

All samples were tested using Nicolet 5700 (Nicolet) with a resolution of 4 cm^{-1}, and the spectra were obtained by 32 scans in the range of 4000–500 cm^{-1}.

Scanning electron microscopy (SEM)

The morphology of PAH was examined using a scanning electron microscope (SEM, Thermo Scientific Apreo 2C) at an acceleration voltage of 10 kV. The samples were treated with liquid nitrogen to obtain cross-sectional fractures, and then the fractures were sputtered with gold axially and radially, respectively.

Swelling test of PAH in H_2O and NaCl(aq.) respectively

Five PAH parallel samples (5 mm × 5 mm × 2 mm) having been dried thoroughly (m_o) were immersed in H_2O and NaCl(aq.) respectively, and the wet weights (m_s) were recorded successively. The swelling ratio (S (%)) for each sample could be calculated using formula (1):

$$S\ (\%) = (m_s - m_o)/m_o \times 100\% \quad (1)$$

Swelling test of PAH in NaCl(aq.) and H_2O alternatively

The PAH specimens (5 mm × 5 mm × 2 mm) were initially immersed in H_2O until reaching an equilibrium (m_e). After that, they were immersed in NaCl(aq.) and H_2O alternatively and the swelling weights $m_{NaCl(N)}$ and $m_{H_2O(N)}$ were obtained. The S(%) in NaCl(aq.) and H_2O in every cycle can be calculated using formulas (2) and (3) respectively:

$$S\ (\%) = (m_{NaCl(N)} - m_e)/m_e \times 100\% \quad (2)$$

$$S\ (\%) = (m_{H_2O(N)} - m_e)/m_e \times 100\% \quad (3)$$

where N signifies the number of cycles (N = 1, 2, 3, 4, 5, and 6).

Adhesion and self-healing tests

The adhesive strength of PAH was investigated using the lap shear test.[31] PAH (10 mm × 10 mm × 2 mm) was stuck in the middle of two plates of plastic, glass and metal substrates respectively. Then, it was pulled by the plates using a universal testing machine (HZ-1004, Lixian Instrument Technology, China) until the two plates separated, and the maximum load was recorded. The adhesive strength was calculated by dividing the measured maximum load by the adhesive area. For self-healing, tensile testing was performed on the universal testing machine, and the modulus of the original sample and that of the healed PAH sample were calculated. For adhesion and self-healing tests, three parallel samples were tested to get the average values.

Conflicts of interest

There are no conflicts to declare.

Acknowledgements

This work was supported by the National Natural Science Foundation of China (51725303 and 52033007), the Sichuan Science and Technology Program (2020YFH0058 and 2022YFSY0017), and the Fundamental Research Funds for the Central Universities (2682022ZTPY039). The authors also thank the Analytical and Testing Center of Southwest Jiaotong University.

References

1 Y. Zhou, X. Dong, Y. Mi, F. Fan, Q. Xu, H. Zhao, S. Wang and Y. Long, *J. Mater. Chem. A*, 2020, **8**, 10007–10025.
2 Y. Ke, J. Chen, G. Lin, S. Wang, Y. Zhou, J. Yin, P. S. Lee and Y. Long, *Adv. Energy Mater.*, 2019, **9**, 1902066.
3 H.-N. Kim and S. Yang, *Adv. Funct. Mater.*, 2020, **30**, 1902597.
4 H. Fan and J. P. Gong, *Macromolecules*, 2020, **53**, 2769–2782.
5 Y. Zhou, Y. Cai, X. Hu and Y. Long, *J. Mater. Chem. A*, 2014, **2**, 13550–13555.
6 X. H. Li, C. Liu, S.-P. Feng and N. X. Fang, *Joule*, 2019, **3**, 290–302.
7 J. E. Stumpel, E. R. Gil, A. B. Spoelstra, C. W. M. Bastiaansen, D. J. Broer and A. P. H. J. Schenning, *Adv. Funct. Mater.*, 2015, **25**, 3314–3320.
8 Y. Wang, R. Shen, S. Wang, Q. Chen, C. Gu, W. Zhang, G. Yang, Q. Chen, Y. M. Zhang and S. X. A. Zhang, *Chem*, 2021, **7**, 1308–1320.
9 L. Wang, X. Jiao, D. Chen and T. Wang, *Adv. Sci.*, 2022, **9**, e2104121.
10 S. Wang, T. Jiang, Y. Meng, R. Yang, G. Tan and Y. Long, *Science*, 2021, **374**, 1501–1504.
11 Y.-S. Yang, Y. Zhou, F. B. Yin Chiang and Y. Long, *RSC Adv.*, 2016, **6**, 61449–61453.
12 R. L. Sala, R. H. Gonçalves, E. R. Camargo and E. R. Leite, *Sol. Energy Mater. Sol. Cells*, 2018, **186**, 266–272.
13 Y. Zhou, M. Layani, S. Wang, P. Hu, Y. Ke, S. Magdassi and Y. Long, *Adv. Funct. Mater.*, 2018, **28**, 1705365.
14 Y. Zhou, S. Wang, J. Peng, Y. Tan, C. Li, F. Y. C. Boey and Y. Long, *Joule*, 2020, **4**, 2458–2474.
15 S. Liu, C. Y. Tso, Y. W. Du, L. C. Chao, H. H. Lee, T. C. Ho and M. K. H. Leung, *Appl. Energy*, 2021, **297**, 117207.
16 L. Tang, L. Wang, X. Yang, Y. Feng, Y. Li and W. Feng, *Prog. Mater. Sci.*, 2021, **115**, 100702.
17 J. Tian, H. Peng, X. Du, H. Wang, X. Cheng and Z. Du, *J. Alloys Compd.*, 2021, **858**, 157725.
18 C. Lin, J. Hur, Y. H. Chao Christopher, G. Liu, S. Yao, W. Li and B. Huang, *Sci. Adv.*, 2022, **8**, eabn7359.
19 Y. Zhou, M. Layani, F. Y. C. Boey, I. Sokolov, S. Magdassi and Y. Long, *Adv. Mater. Technol.*, 2016, **1**, 1600069.
20 H. Fang, P. Zheng, R. Ma, C. Xu, G. Yang, Q. Wang and H. Wang, *Mater. Horiz.*, 2018, **5**, 1000–1007.
21 J. L. Wang, S.-Z. Sheng, Z. He, R. Wang, Z. Pan, H. Y. Zhao, J. W. Liu and S. H. Yu, *Nano Lett.*, 2021, **21**, 9976–9982.
22 P. V. Rathod, P. P. More, J. M. C. Puguan and H. Kim, *Sol. Energy Mater. Sol. Cells*, 2021, **230**, 111202.
23 C. Yu, H. Guo, K. Cui, X. Li, Y. N. Ye, T. Kurokawa and J. P. Gong, *Proc. Natl. Acad. Sci. U. S. A.*, 2020, **117**, 18962–18968.
24 T. L. Sun, T. Kurokawa, S. Kuroda, A. B. Ihsan, T. Akasaki, K. Sato, M. A. Haque, T. Nakajima and J. P. Gong, *Nat. Mater.*, 2013, **12**, 932–937.
25 F. Luo, T. L. Sun, T. Nakajima, T. Kurokawa, A. B. Ihsan, X. Li, H. Guo and J. P. Gong, *ACS Macro Lett.*, 2015, **4**, 961–964.
26 F. Luo, T. L. Sun, T. Nakajima, T. Kurokawa, Y. Zhao, K. Sato, A. B. Ihsan, X. Li, H. Guo and J. P. Gong, *Adv. Mater.*, 2015, **27**, 2722–2727.
27 J. Yang, T. Lim, S. M. Jeong and S. Ju, *ACS Appl. Mater. Interfaces*, 2021, **13**, 20689–20697.
28 T. Nakamura, Y. Takashima, A. Hashidzume, H. Yamaguchi and A. Harada, *Nat. Commun.*, 2014, **5**, 4622.
29 H. Lee, D.-S. Um, Y. Lee, S. Lim, H. J. Kim and H. Ko, *Adv. Mater.*, 2016, **28**, 7457–7465.
30 L. Liu, Z. Liu, Y. Ren, X. Zou, W. Peng, W. Li, Y. Wu, S. Zheng, X. Wang and F. Yan, *Angew. Chem., Int. Ed.*, 2021, **60**, 8948–8959.
31 X. Chen, J. Zhang, G. Chen, Y. Xue, J. Zhang, X. Liang, I. M. Lei, J. Lin, B. B. Xu and J. Liu, *Adv. Funct. Mater.*, 2022, **32**, 2202285.
32 A. B. Ihsan, T. L. Sun, T. Kurokawa, S. N. Karobi, T. Nakajima, T. Nonoyama, C. K. Roy, F. Luo and J. P. Gong, *Macromolecules*, 2016, **49**, 4245–4252.
33 S. Wu, Z. Shao, H. Xie, T. Xiang and S. Zhou, *J. Mater. Chem. A*, 2021, **9**, 1048–1061.